3D Representation Models Construction through a Volume Geometric Decomposition Method

Gisele Simas, Rodrigo de Bem and Silvia Botelho
Centro de Ciências Computacionais (C3), Universidade Federal do Rio Grande (FURG),
Av. Itália, km 8, 96203-900, Rio Grande, RS, Brazil

Keywords: Representation Model, Volumetric Reconstruction, 3D Motion Tracking.

Abstract: Despite the fact of 3D motion tracking has being highly explored in the computer vision researches, it still faces some relevant challenges, such as the tracking of objects using few a priori knowledge. In this context, this work presents the Volume Geometric Decomposition method, capable of constructing representation models of distinct and previously unknown objects. This method is executed over a probabilistic volumetric reconstruction of the interested objects. It adjusts the representation to the reconstructed volume, minimizing the amount of empty space enclosed by the model. Such representation model is composed by an appearance and a kinematic models. The former is comprised of ellipsoids and joints, while the latter is implemented through the *Loose-Limbed model*, a probabilistic graphical model. The performed experiments and the obtained results shown that the proposed method successfully constructed representation models to highly distinct and a priori unknown objects.

1 INTRODUCTION

The 3D motion tracking has being highly explored in the computer vision researches. Realistic results are already achieved specifically in human motion tracking (Sigal and Black, 2010). However, the tracking methods still have certain limitations. In order to reduce these restrictions, in recent years, greater attention has being devoted to obtaining more general methods that allow: motion tracking from monocular images (Fossati et al., 2009); use of unsynchronized moving cameras (Hasler et al., 2009); the exemption from manual initialization (Sundaresan and Chellappa, 2009); adaptation to different forms of the same object (Mikić et al., 2003); online processing of modifications (Ross et al., 2008); motion tracking of distinct objects (Ukita et al., 2009); reduction of the needed amount of a priori information (Gall et al., 2010).

The overcome of some restrictions passes through the use of more general and flexible representation models. In the context of motion tracking frameworks, the representation models are employed to model the tracking objects, gathering relevant information about their structure and appearance. According to Caillette (Caillette, 2006), the representation models can be classified as: **i) appearance models**: describe properties of the objects' parts, such as shape and color; **ii) kinematic models**: describe the kinematical relations between the objects' parts, establishing spacial relations and movement rules through them; **iii) dynamic models**: describe the mechanical properties of the objects' parts, considering their masses, sizes and forces.

Representation models are employed in many applications, such as animation (Starck and Hilton, 2007), motion capture (Gall et al., 2010), segmentation (Mian et al., 2006), object recognition (Toshev et al., 2009) and motion synthesis (Huang et al., 2009). This is possible because model based approaches allow the representation of distinct objects, the gathering of visual, structural and mechanical objects' properties, and the representation of distinct poses of objects.

Thus, this work proposes a novel approach for automatic representation model construction of distinct and a priori unknown objects. This method is part of a markerless 3D motion tracking framework, based on probabilistic volumetric reconstruction, which has the goal of tracking distinct targets using as few a priori knowledge as possible. Into the present approach, the representation model is composed by an appearance model and by a kinematic model. These are adjusted to the objects volumetric reconstruction through the

Simas G., de Bem R. and Botelho S..
3D Representation Models Construction through a Volume Geometric Decomposition Method.
DOI: 10.5220/0004288502740279
In *Proceedings of the International Conference on Computer Vision Theory and Applications* (VISAPP-2013), pages 274-279
ISBN: 978-989-8565-48-8
Copyright © 2013 SCITEPRESS (Science and Technology Publications, Lda.)

Volume Geometric Decomposition method, that decomposes the occupied volume aiming to minimize the amount of unoccupied voxels inside the representation model. The obtained results shown that the proposed approach was capable of constructing models of different kinds of objects, articulated or not, adjusting adequately to their shapes and rigid parts. Doing so, this method contributes in the direction of more general and flexible 3D motion tracking approaches.

2 RELATED WORK

The appearance and kinematic models are the most usual models employed in motion tracking approaches. Appearance models are usually composed by sets of geometric shapes, such as, ellipsoids (Caillette, 2006), truncated quadrics (Cipolla et al., 2003) and truncated cones (Darby et al., 2008); or even by polygonal meshes (Gall et al., 2010). Mostly kinematic models are formed by kinematic chains, composed by links (rigid parts) and joints (connections between the rigid parts) (Caillette, 2006), (Canton-Ferrer et al., 2009), (Gall et al., 2010). Usually restrictions are associated to the kinematic models to rule their possible poses. Databases with movements of objects are employed in some approaches to allow the learning of such restrictions (Gall et al., 2010).

Most 3D motion tracking methods employ predefined representation models or adaptable models to different forms of the same object type (Mikić et al., 2003), (Starck and Hilton, 2003). Usually, the object appearance model is associated with the object kinematic model that describes the possible movements and valid poses (Canton-Ferrer et al., 2009). A few techniques are dedicated to automatic and unsupervised construction of representation models. The existing approaches build models by establishing correspondences in a sequence of images of the objects in different poses, using local features (Ross et al., 2010), (Song et al., 2003) and optical markers (de Aguiar et al., 2006); establishing correspondences between vertices of a priori known mesh (de Aguiar et al., 2008), (Anguelov et al., 2004), (James and Twigg, 2005), (Schaefer and Yuksel, 2007); clustering and applying heuristics to match objects' rigid parts over time (de Aguiar et al., 2004), (Theobalt et al., 2004). In some proposals, the models learned can be interpreted as containing certain temporal coherence, obtained by the constraints defined in the establishment of the correspondences (Theobalt et al., 2004). Few methodology perform some motion estimation in conjunction with the estimation of the objects representation model (Ross et al., 2010).

3 3D MOTION TRACKING FRAMEWORK

The present methodology is proposed in the context of a 3D motion tracking framework. This framework is composed by four main parts: an *observation model*, a *representation model*, a *movement model* and a *motion tracking methodology*. The *observation model* defines which kind of sensory information about the interested objects is extracted from the environment. In the present framework the environment is sensored by multiple synchronized and calibrated cameras which capture images used to build a probabilistic volumetric reconstruction of the interested objects (Franco and Boyer, 2005). This reconstruction is performed in a 3D grid composed by voxels, which present a probability to be occupied or not. The *representation model* defines how the interested objects are 'seen' into the motion tracking framework. This model will be detailed in the present work. The *movement model* defines how the sensored objects move along the time. In this framework there is no a priori information about the movements of the objects. Finally, the *tracking methodology* is the technique employed to gather all these models and follow the targets (objects) in the 3D space along the time.

4 REPRESENTATION MODEL

The employed representation model consists of an *appearance model* and a *kinematic model*. The *appearance model* represents the dimensions and shapes of the objects' rigid parts. In this work, a set of ellipsoids was adopted. These geometric shapes enclose the occupied voxels belonging to objects' rigid parts. Each ellipsoid is represented by a centroid $\vec{C}$ and three vectors $\vec{a}$, $\vec{b}$ and $\vec{c}$, representing their principal axes. These vectors define the size and the orientation of each ellipsoid. A joint J is defined between every two ellipsoids E_1 and E_2 that appear to be connected. This connection is established between ellipsoids that enclose neighbor voxels. Two vectors, $\vec{v_1}$ and $\vec{v_2}$, link the joint J to the centroid of the connected ellipsoids. The ellipsoids and the joints are illustrated in Figure 1.

As the objects to be represented are not known a priori, the use of a predefined kinematic model is not appropriated. Instead of the imposition of static and previously defined kinematic restrictions, a flexible approach is needed. Thus, the *Loose-Limbed model* (Sigal et al., 2003) was employed. Into this model an object is represented as a probabilistic graphical model. The nodes of such model correspond to the

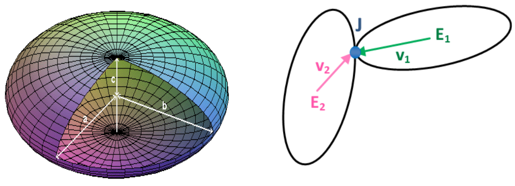

(a) (b)

Figure 1: *Appearance model* - (a) ellipsoidal geometric shape; (b) joint *J* between two connected ellipsoids (2D simplified representation).

objects' rigid parts (ellipsoids), while the edges correspond to the connections between such parts (joints). Applying this model over the appearance model turns the deterministic ellipsoids' positions, orientations and connections into flexible probabilistic beliefs. An example of Loose-Limbed model can be seen in Figure 2.

Sigal (Sigal et al., 2003) compare this model with a ”toy push puppet” with elastic joints: one part of the object pulls and pushes the adjacent parts, but them does not need to be exactly glued. Thus, certain flexibility is achieved, however the object movements are still restricted. This model allows, in the context of motion tracking, changes over the objects' parts connections. Corrections in the representation model are possible when, for instance, two parts are erroneously considered dependent on a first moment, and found not physically connected in a second instant. The vice-versa situation can also be corrected.

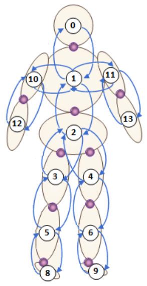

Figure 2: Probabilistic graphical model - rigid parts and their connections.

5 VOLUME GEOMETRIC DECOMPOSITION METHOD

This method constructs representation models of distinct and a priori unknown objects from a volumetric reconstruction of them. It divides the set of occupied voxels in geometric shapes (ellipsoids, in the present proposal), so that, within each shape, a minimum quantity of empty space remains. Firstly, a connected component (connected group of voxels) is identified through a breadth-first search; next, the voxels position mode of this component is calculated; then an ellipsoid is expanded from the voxel nearest to the position mode, so that the percentage of unoccupied voxels (not occupied by any object) within the ellipsoid is kept as small as possible. The found ellipsoid must enclose a minimum number of occupied voxels to be considered as a valid object's part, otherwise it is disregarded. The process is repeated until all voxels have been analyzed. Algorithm 1 shows the method pseudo-code and their main subroutines are detailed in the next subsections.

Algorithm 1: A Volume Geometric Decomposition.

```
While there is non analyzed voxels
    Identify Connected Component of voxels
    Identify the Nearest Voxel to the connected component position mode
    Expand a New Ellipsoid from the nearest voxel
    Mark the already analyzed voxels
    If the number of ellipsoid's voxels > threshold
        Accept the new ellipsoid
    Else
        Discard the new ellipsoid
    End If
End While
```

a) Identify Connected Component: from a non analyzed and occupied voxel v this subroutine executes a breadth-first search for voxels that fulfill the following requisites: i) to be occupied; ii) not to be previously analyzed; iii) not to be associated to any other ellipsoid. All the connected voxels that meet these conditions are assigned to the same connected component.

b) Identify the Nearest Voxel: into this subroutine the position mode M_o of the voxels connected component is calculated[1] and after that, the nearest voxel is identified. The mode was chosen among the geometric center and the median of the volume because it was the most effective to kept the ellipsoid's center way from volume borders.

c) Expand a New Ellipsoid: In order to expand a new ellipsoid, firstly, is defined that only the occupied voxel closest to the mode belongs to the ellipsoid. Then, a breadth-first search is performed from this voxel, adding one level of the search at a time. At each new added level, the ellipsoid that covers all the added occupied voxels is recalculated. Next, all the occupied voxels that are inside the obtained shape

[1] The mode is separately calculated for each dimension x, y and z.

SCITEPRESS SCIENCE AND TECHNOLOGY PUBLICATIONS

SCITEPRESS SCIENCE AND TECHNOLOGY PUBLICATIONS

and that have not yet been assigned to any ellipsoid are also associated. Then, the new central voxel of the ellipsoid is determined. This is employed to move the center of the ellipsoid to a position more favorable to their growth (thus, the ellipsoid moves toward the object volume and, consequently, it can include a greater number of voxels). The process is continued until the ellipsoid stops to grown for a certain number of iterations or whether it became invalid. An ellipsoid is considered invalid if this rate of empty voxels within the shapes is greater than a certain threshold. The two subroutines that compose the process are detailed in the following subsections.

c.1) Update Ellipsoid's Parameters: this method receives a set of occupied voxels V_E and calculates the shape of the ellipsoid E that encloses those voxels. Initially, the mean position and the covariance matrix are calculated. Next, the singular value decomposition of the covariance matrix is employed to obtain the principal axes of the ellipsoid ($\vec{a}$, $\vec{b}$ e $\vec{c}$). The eigenvectors of the covariance matrix correspond to the directions of the axes and the eigenvalues correspond to the modules of these axes (Banégas et al., 2001).

c.2) Check Ellipsoid's Validity: the obtained ellipsoid must present a minimal size in each one of their principal axes. To correct the shapes in which the covariance matrix has not this minimal variation in the direction of the main axes, new values are assigned to the axes considered inappropriated. Three cases are considered according to the number of axes which have module less than the threshold:

1. three axes - a standard ellipsoid with minimum size is assigned;
2. two axes - only the direction and the module of one axis is known, so let $\vec{A}$ be the known axis, the other two axes must be orthogonal to $\vec{A}$ and between themselves. An arbitrary vector $\overrightarrow{ncol_A}$ is calculated. Then, from the cross product, $\vec{B} = \vec{A} \times \overrightarrow{ncol_A}$, a vector $\vec{B}$ orthogonal to $\vec{A}$ is obtained. The third vector is obtained as $\vec{C} = \vec{A} \times \vec{B}$;
3. one axis - let $\vec{A}$ and $\vec{B}$ be the known axes, the direction of the unknown axis is given by $\vec{C} = \vec{A} \times \vec{B}$.

A final ellipsoid's parameters adjustment is required, specially when the voxels are not uniformly distributed inside the shape. This adjustment changes the main axes modules, but not their directions previously obtained. To do so, the rotation matrix that aligns the ellipsoid principal axes parallel to the coordinate axes is calculated. The same rotation is applied to the position vectors $\overrightarrow{P_v}$ of each voxel v inside the ellipsoid E, obtaining the vectors $\overrightarrow{P_{vr}}$. The constants a, b and c are calculated as follow:

$$\begin{aligned} a &= (maximum(P_{vr_x}) - minimum(P_{vr_x}))/2, \\ b &= (maximum(P_{vr_y}) - minimum(P_{vr_y}))/2, \\ c &= (maximum(P_{vr_z}) - minimum(P_{vr_z}))/2, \end{aligned} \tag{1}$$

where *maximum* and *minimum* concerns all voxels values. Finally, we define the module of the new principal axes of the ellipsoid ($\vec{a_n}$, $\vec{b_n}$ e $\vec{c_n}$) as follows:

$$\vec{a_n} = a * \frac{\vec{a}}{|\vec{a}|}, \quad \vec{b_n} = b * \frac{\vec{b}}{|\vec{b}|}, \quad \vec{c_n} = c * \frac{\vec{c}}{|\vec{c}|}. \tag{2}$$

6 EXPERIMENTS AND RESULTS

The experiments were performed with three different image sequences, obtained in a public benchmark dataset (Inria, 2012). Each one of the sequences is composed by images captured by multiple synchronized and calibrated cameras along a period of time. From a set of images, captured at the same time instant, a probabilistic volumetric reconstruction is built (Franco and Boyer, 2005). The objects representation model is then constructed over this volumetric reconstruction through the Volume Geometric Decomposition method. Samples of the images sequences are shown in the Figure 3, while samples of the volumetric reconstruction is shown in the Figure 4.

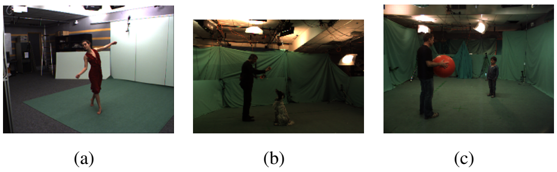

Figure 3: Samples of the benchmark image sequences *Dance*, *Dog* and *Child*. Each sequence was captured by 8, 16 and 16 cameras, respectively, during a period of time. (a) One of the eight images from the *Dance* sequence. (b) One of the sixteen images from the *Dog* sequence. (c) One of the sixteen images from the *Child* sequence.

The Figures 5, 6 and 7 presents the representation models for the time instant $t = 0$ of the sequence *Dance*, *Dog* and *Child*, respectively. The minimum size of the ellipsoids was equal to 15 voxels, while the threshold for the accepted rate of unoccupied voxels enclosed by the shapes was 0.3.

The presented results shown the construction of representation models for different kinds of objects: adult humans, a child, a dog and balls. Such benchmark is considered by the authors sufficiently general to test the proposed method, intended to be capable of building representation models for distinct and a priori unknown objects.

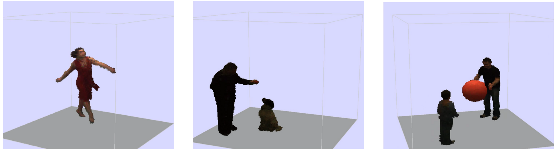

(a) (b) (c)

Figure 4: Samples of probabilistic volumetric reconstruction of the benchmark sequences (a) *Dance*, (b) *Dog* and (c) *Child*.

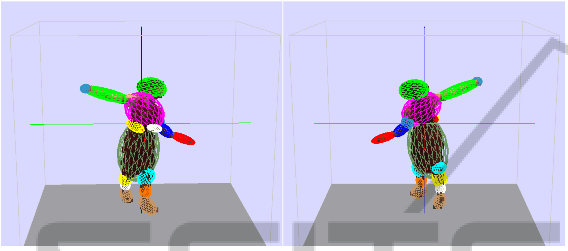

Figure 5: Representation model obtained by Volume Geometric Decomposition method. Image sequence *Dance* at time $t = 0$ - the ellipsoids are expanded from the connected components modes.

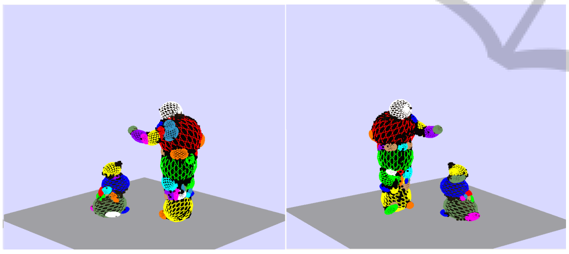

Figure 6: Representation model obtained by Volume Geometric Decomposition method. Image sequence *Dog* at time $t = 0$ - the ellipsoids are expanded from the connected components modes.

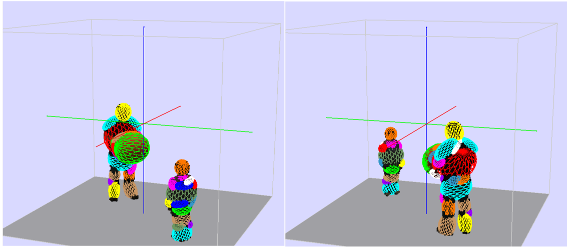

Figure 7: Representation model obtained by Volume Geometric Decomposition method. Image sequence *Child* at time $t = 0$ - the ellipsoids are expanded from the connected components modes.

It can be seen that the Volume Geometric Decomposition method could successfully built the representation model to all objects in the sequences, adjusting the ellipsoids to the volumetric reconstruction and keeping the number of unoccupied voxels inside the geometric shapes as small as possible. The method could correctly identify some objects' rigid parts, as the humans' and dog's heads, the humans' thoraces and the ball. In other points, as the arms of the dancer (Figure 5), the method correctly identified two rigid parts in the left arm, but erroneously detected the right arm as just one rigid object. The child, in the *Child* sequence (Figure 7), and the man, in the *Dog* sequence (Figure 6), appear with their legs put together, what generates some noise in the volumetric reconstruction and consequently the existence of many small ellipsoids representing that volumes.

7 CONCLUSIONS

This work present as the main contribution a novel method, named Volume Geometric Decomposition, to the automatic construction of objects representation models from volumetric reconstructions, in the context of a 3D motion tracking framework. The employed representation model is composed by an *appearance model* and a *kinematic model*. The former is comprised of ellipsoids and joints, while the latter is implemented through a *Loose-Limbed model*, a probabilistic graphical model, which turns the deterministic position and orientation parameters of the ellipsoids and joints into probabilistic beliefs.

The Volume Geometric Decomposition method adjusts the ellipsoids to the volumetric reconstruction and kept the number of unoccupied voxels inside the geometric shapes as small as possible. As could be seen in the results of the experiments, the method successfully achieved this goal. It was capable of representing all objects volumes. Despite some rigid parts and joints have not been correctly identified, the adopted Loose-Limbed model approach aims, in the context of the motion tracking framework, the posterior refinement of the initially found representation models. This could be accomplished by the use of the Nonparametric Belief Propagation (NBP) technique (Sudderth et al., 2003), (Sudderth et al., 2010) and the PArticle Message PASsing (PAMPAS) algorithm (Isard, 2003).

As future works, some points must be explored. A quantitative metric to evaluate the representation model quality, in terms of volume representation, is desired. The comparison between this approach and clustering algorithms is also highly recommended. Finally, the refinement of the representation models, through the NBP and PAMPAS algorithms is extremely important, once it justifies the Loose-Limbed model adoption.

SCITEPRESS SCIENCE AND TECHNOLOGY PUBLICATIONS

REFERENCES

Anguelov, D., Koller, D., Pang, H.-C., Srinivasan, P., and Thrun, S. (2004). Recovering articulated object models from 3d range data. In *20th Conf. on Uncertainty in Artificial Intelligence*, UAI '04, pages 18–26.

Banégas, F., Jaeger, M., Michelucci, D., and Roelens, M. (2001). The ellipsoidal skeleton in medical applications. In *Sixth ACM Symp. on Solid Modeling and Appl.*, SMA '01, pages 30–38.

Caillette, F. (2006). *Real-Time Markerless 3D Human Body Tracking*. Phd thesis, University of Manchester.

Canton-Ferrer, C., Casas, J., and Pardas, M. (2009). Voxel based annealed particle filtering for markerless 3d articulated motion capture. In *3DTV Conf.: The True Vision - Capture, Transmission and Display of 3D Video, 2009*, pages 1 –4.

Cipolla, R., Stenger, B., Thayananthan, A., and Torr, P. (2003). Hand tracking using a quadric surface model and bayesian filtering. In *Mathematics of Surfaces*, volume 2768 of *LNCS*, pages 129–141. Springer.

Darby, J., Li, B., and Costen, N. (2008). Behaviour based particle filtering for human articulated motion tracking. In *ICPR, 2008*, pages 1–4.

de Aguiar, E., Theobalt, C., Magnor, M., Theisel, H., and Seidel, H.-P. (2004). M3: marker-free model reconstruction and motion tracking from 3d voxel data. In *Pacific Graphics, 2004*, pages 101–110.

de Aguiar, E., Theobalt, C., and Seidel, H.-P. (2006). Automatic learning of articulated skeletons from 3d marker trajectories. In *Second Int. Conf. on Advances in Visual Computing*, ISVC'06, pages 485–494.

de Aguiar, E., Theobalt, C., Thrun, S., and Seidel, H.-P. (2008). Automatic conversion of mesh animations into skeleton-based animations. *Computer Graphics Forum*, 27(2):389–397.

Fossati, A., Salzmann, M., and Fua, P. (2009). Observable subspaces for 3d human motion recovery. In *CVPR, 2009*, pages 1137–1144.

Franco, J.-S. and Boyer, E. (2005). Fusion of multiview silhouette cues using a space occupancy grid. In *ICCV, 2005*, pages 1747–1753.

Gall, J., Rosenhahn, B., Brox, T., and Seidel, H.-P. (2010). Optimization and filtering for human motion capture. *Int. J. of Computer Vision*, 87:75–92.

Hasler, N., Rosenhahn, B., Thormahlen, T., Wand, M., Gall, J., and Seidel, H.-P. (2009). Markerless motion capture with unsynchronized moving cameras. In *CVPR, 2009*, pages 224–231.

Huang, P., Hilton, A., and Starck, J. (2009). Human motion synthesis from 3d video. In *CVPR, 2009*, pages 1478–1485.

Inria (2012). 4d repository. *Perception Group, Inria Rhône-Alpes. http://4drepository.inrialpes.fr.*

Isard, M. (2003). Pampas: real-valued graphical models for computer vision. In *CVPR, 2003*, pages 613–620.

James, D. L. and Twigg, C. D. (2005). Skinning mesh animations. *ACM Trans. Graph.*, 24(3):399–407.

Mian, A., Bennamoun, M., and Owens, R. (2006). Three-dimensional model-based object recognition and segmentation in cluttered scenes. *IEEE Trans. Pattern Anal. Machine Intell.*, 28(10):1584 –1601.

Mikić, I., Trivedi, M., Hunter, E., and Cosman, P. (2003). Human body model acquisition and tracking using voxel data. *Int. J. of Computer Vision*, 53:199–223.

Ross, D., Lim, J., Lin, R.-S., and Yang, M.-H. (2008). Incremental learning for robust visual tracking. *Int. J. of Computer Vision*, 77:125–141.

Ross, D., Tarlow, D., and Zemel, R. (2010). Learning articulated structure and motion. *Int. J. of Computer Vision*, 88:214–237.

Schaefer, S. and Yuksel, C. (2007). Example-based skeleton extraction. In *Fifth Eurographics Symp. on Geometry Processing*, SGP '07, pages 153–162.

Sigal, L. and Black, M. (2010). Guest editorial: State of the art in image- and video-based human pose and motion estimation. *Int. J. of Computer Vision*, 87:1–3.

Sigal, L., Isard, M., Sigelman, B. H., and Black, M. J. (2003). Attractive people: Assembling loose-limbed models using non-parametric belief propagation. In *NIPS, 2003*, pages 1539–1546.

Song, Y., Goncalves, L., and Perona, P. (2003). Unsupervised learning of human motion. *IEEE Trans. Pattern Anal. Machine Intell.*, 25(7):814 – 827.

Starck, J. and Hilton, A. (2003). Model-based multiple view reconstruction of people. In *ICCV, 2003*, pages 915–922.

Starck, J. and Hilton, A. (2007). Surface capture for performance-based animation. *IEEE Comput. Graph. Appl.*, 27:21–31.

Sudderth, E., Ihler, A., Freeman, W., and Willsky, A. (2003). Nonparametric belief propagation. In *CVPR, 2003.*, pages 605–612.

Sudderth, E. B., Ihler, A. T., Isard, M., Freeman, W. T., and Willsky, A. S. (2010). Nonparametric belief propagation. *Commun. ACM*, 53(10):95–103.

Sundaresan, A. and Chellappa, R. (2009). Multicamera tracking of articulated human motion using shape and motion cues. *IEEE Trans. on Image Processing*, 18(9):2114 –2126.

Theobalt, C., de Aguiar, E., Magnor, M. A., Theisel, H., and Seidel, H.-P. (2004). Marker-free kinematic skeleton estimation from sequences of volume data. In *ACM Symp. on Virtual Reality Software and Technology, 2004*, VRST '04, pages 57–64. ACM.

Toshev, A., Makadia, A., and Daniilidis, K. (2009). Shape-based object recognition in videos using 3d synthetic object models. In *CVPR, 2009*, pages 288 –295.

Ukita, N., Hirai, M., and Kidode, M. (2009). Complex volume and pose tracking with probabilistic dynamical models and visual hull constraints. In *ICCV, 2009*, pages 1405 –1412.

SCITEPRESS SCIENCE AND TECHNOLOGY PUBLICATIONS